PHYSICAL REVIEW B VOLUME 51, NUMBER 9 1 MARCH 1995-I

Reversible magnetization, critical fields, and vortex structure in grain-aligned $YBa_2Cu_4O_8$

Junghyun Sok, Ming Xu, Wei Chen, B. J. Suh, J. Gohng,*
D. K. Finnemore, and M. J. Kramer
Ames Laboratory, U.S. Department of Energy and Department of Physics and Astronomy, Iowa State University, Ames, Iowa 50011

L. A. Schwartzkopf
Department of Physics, Mankato State University, Mankato, Minnesota 56002

B. Dabrowski
Department of Physics, Northern Illinois University, Dekalb, Illinois 60115
(Received 20 October 1994)

Reversible-magnetization data have been studied for $YBa_2Cu_4O_8$ in order to determine the thermodynamic properties and the magnetic-field dependence of the superfluid density. By fitting the Hao-Clem variational model to the reversible magnetization data below T_c, superconducting parameters such as the Ginzburg-Landau parameter κ, the thermodynamic critical field H_c, and the superconducting order parameter are determined. The upper and lower critical fields H_{c2}, H_{c1}, the penetration depth λ, and the coherence length ξ are derived. Within the model there is a direct connection between the magnetization and the superfluid density, so the vortex structure, the behavior of the average order parameter in (H,T) plane, and the magnetic-field dependence of the superfluid density are obtained. In the high-field region, the evidence of strong vortex fluctuation effects is observed and explained by vortex fluctuation for a three-dimensional superconductor. The mean-field transition temperature $T_c(H)$ and dH_{c2}/dT near T_c derived from the analysis of vortex fluctuation effects are comparable with fitting results.

I. INTRODUCTION

The Hao-Clem theory has proven to be remarkably successful in describing the thermodynamic properties of $YBa_2Cu_3O_7$ (Y-123). There are several different regimes of temperature and magnetic field with different models applicable. The Ginzburg-Landau (GL) theory is the fundamental pioneering work for isotropic classical superconductors that applies in the limit that the superconducting order parameter is not too large near T_c.[1] In the GL theory, a complex pseudowave function Ψ is introduced as an order parameter for the superconducting electrons and the free energy is expressed as a function of the order parameter and magnetic field. Both of these two variational parameters are used to minimize the free energy. For the high-field region $H_{c2} - H \ll H_{c2}$, the Abrikosov solution[2] based on the GL equations is applicable by using the fact that $|\Psi|^2$ is small near H_{c2} to solve the GL equations perturbatively, where $|\Psi|$ is the amplitude of the order parameter. The Abrikosov result, however, gives a static array of vortices and hence is not applicable to the high-T_c superconductors[3] where flux line lattice melting, entangled vortex structures, vortex glass behavior, and strong fluctuation effects occur. For the intermediate field $H_{c1} \ll H \ll H_{c2}$ which most experimental magnetization data fall into, the London model[1] provides the detailed phenomenological description for extreme type-II superconductors for which the GL parameter $\kappa = \lambda/\xi$ satisfies $\kappa \gg 1$, where λ is the penetration depth and ξ is the coherence length. In the London model, both the magnetic flux density and the supercurrent density of an isolated vortex diverge on the axis of the vortex, because the vortex core is ignored, where the order parameter suppresses to zero. Recently, Hao and Clem[4,5] developed a variational model that includes an energy term arising from suppression of the order parameter in the vortex core. They then solved the GL-like equation numerically in the intermediate region. Successful application[4,6] of the Hao-Clem model to the experimental $M(H)$ data allows the GL parameter κ and the critical field H_c to be determined as fitting parameters to a variational solution for an extreme type-II superconductor, where the GL parameter satisfies the condition $\kappa \gg 1$ in the reversible magnetization regime.

The $YBa_2Cu_4O_8$ (Y-124) structure is closely related to the Y-123 structure, except with one additional Cu-O chain per unit cell, that is, Y-124 has two CuO_2 planes and two CuO chains in the unit cell. This leads to a longer c-lattice parameter of 27.21 Å. Y-124 is characterized by an excellent thermal stability of the oxygen content, while Y-123 is strongly sensitive to the oxygen concentration changes that occur as crystals are cooled in different partial pressures of oxygen.[7] Although Y-124 is a good candidate for applications, there has been an

ambiguity in experimental determinations of fundamental physical parameters, such as the GL parameter κ, critical fields, and penetration depth among published results.[8,9]

In this paper, we applied the Hao-Clem model to the reversible magnetization data in order to determine the superconducting physical parameters. Because the data fit the model well, a rather detailed picture of the vortex structure and the magnetic-field dependence of the average order parameter for a given temperature can be derived. A universal curve when plotted on the average of the square of the order parameter vs the H/H_{c2} plot as predicted in theory[10] can be obtained. Finally, the analysis of strong vortex fluctuation was carried out at higher temperatures where fluctuation models apply.

II. EXPERIMENT

About a 10-g polycrystalline sample of Y-124 was synthesized from a stoichiometric mixture of oxide of Y and Cu, and barium carbonate in air at 900 °C. The sample was fired several times with frequent intermediate grindings until no trace of barium carbonate could be detected in the x-ray diffraction pattern. A subsequent high pressure synthesis was done three times for 12 h in 20% O_2 in argon at a total pressure of 2 Kbar (600 atm O_2 pressure) at 1050 °C followed by slow cooling (1.5 deg/min) to room temperature. A large capacity hot isostatic press system (inside diameter = 8 cm and height = 16 cm) was used for high oxygen pressure synthesis.

Grain-aligned powders of tiny single crystals were used instead of one single crystal in order to give a larger sample and a better signal-to-noise ratio. To make a grain-aligned sample in an epoxy matrix, the bulk pellets were ground to a powder of an average diameter 12–20 μm and mixed thoroughly with a low viscosity and low magnetic susceptibility out-gassed epoxy (EPOTEK 301) in a Teflon container. The liquid slurry was placed in magnetic fields of 8.2 T for 15 h. A flat-plate sample was prepared for the x-ray diffraction studies to test whether the c axis of the grain-aligned sample is perpendicular to the surface of the plate. Cylindrical samples were made in the same container for magnetization measurements.

The x-ray diffraction patterns of θ–2θ scan for an aligned sample with the c axis perpendicular to the surface is shown in Fig. 1. The *(0,0,l)* lines are very strongly enhanced by the alignment, and the other lines are suppressed into the noise level. To obtain a more quantitative measure of the mosaic spread of the grains, a pole figure experiment indicates that the full width of half maximum for the *(0,0,*14) peak, FWHM, is about 1.8°. This value for the grain-aligned Y-124 is the same as the typical values for Y-123.

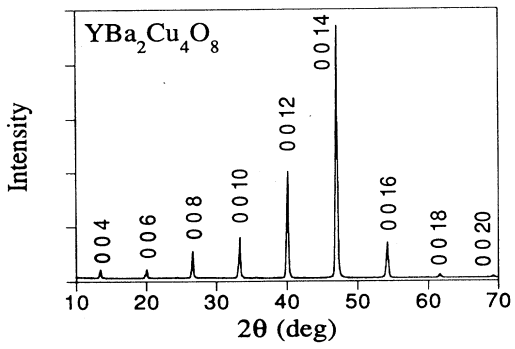

FIG. 1. X-ray data for c-axis grain-aligned bulk Y-124, identifying all of the major peaks.

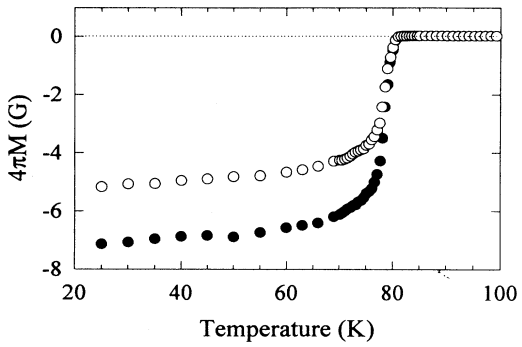

FIG. 2. The magnetic shielding (ZFC) and Meissner effect (FC) measurements of c-axis grain-aligned Y-124 for 5 Oe applied parallel to the c axis.

All the magnetization measurements were carried out in a magnetic field applied parallel to the c axis with use of a superconducting quantum interference device (SQUID). A 3-cm scan length was used for the field homogeneity. Both the shielding and Meissner data for the aligned sample taken at a magnetic field of 5 Oe is shown in Fig. 2, with the onset transition temperature of 81.4 K. The correction for background was made by extrapolation of a linear fit to the normal state data between 100 and 250 K.

III. RESULTS AND DISCUSSION

A. Determination of superconducting parameters

The analysis presented here is based on a fit of $M(H)$ data constructed from a series of $M(T)$ data at various applied magnetic fields parallel to the c-axis in the reversible regime to the Hao-Clem model. Figure 3(a) shows the fitting results of the magnetization data for the various temperatures between 68 and 74 K. As the temperature approaches 74 K, the magnetization data show small deviations from the fitting line near the high-field range because the strong fluctuation effects become important in this range. The data have been fitted two ways, first by forcing κ to be the average κ value, 70, and then by allowing κ to be a free parameter. With κ forced to be 70, all the magnetization data of Fig. 3(a) collapse to a single curve shown in Fig. 3(b). If κ is allowed to be a free variable, one obtains the temperature dependent κ shown in Fig. 4 where κ varies from 69 to 72. If data above 74 K are used, κ begins to increase as expected for

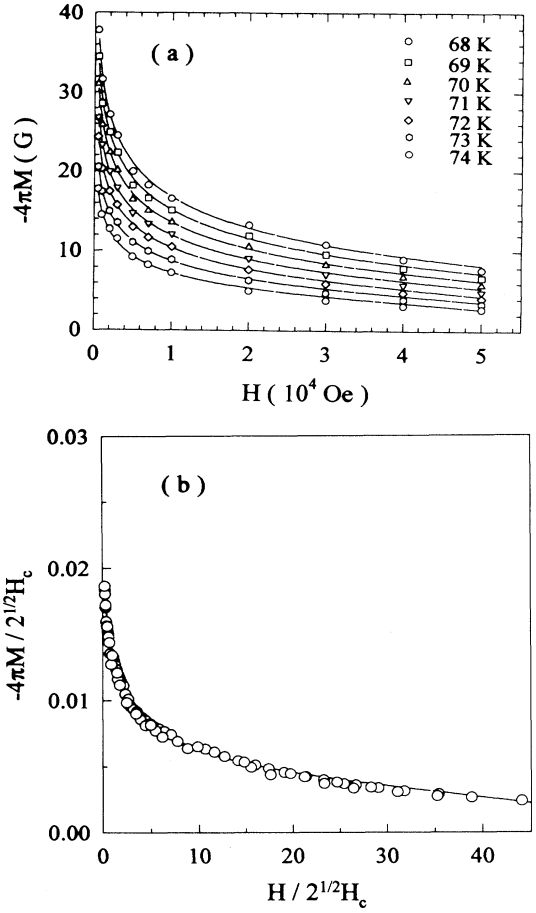

FIG. 3. (a) shows the results of the Hao-Clem fitting to the magnetization data for all temperatures between 68 K and 74 K. (b) shows a scaling behavior in dimensionless units with the average $\kappa = 70$ and $\sqrt{2}H_c(T)$ for the same range of temperature in (a). Solid lines are fitting results.

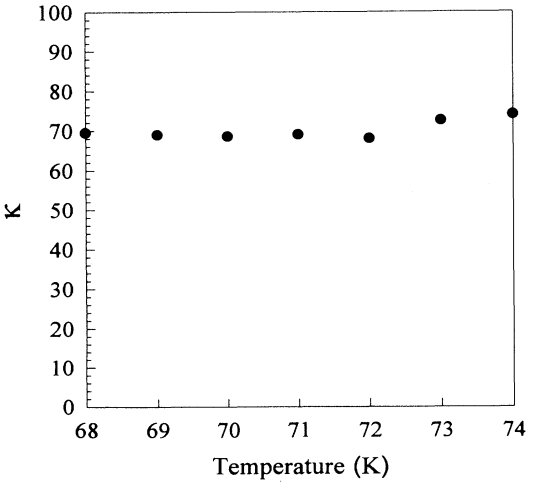

FIG. 4. The temperature dependence of the GL parameter κ, derived from the Hao-Clem fitting to magnetization data $M(H)$ with the magnetic field parallel to the c axis.

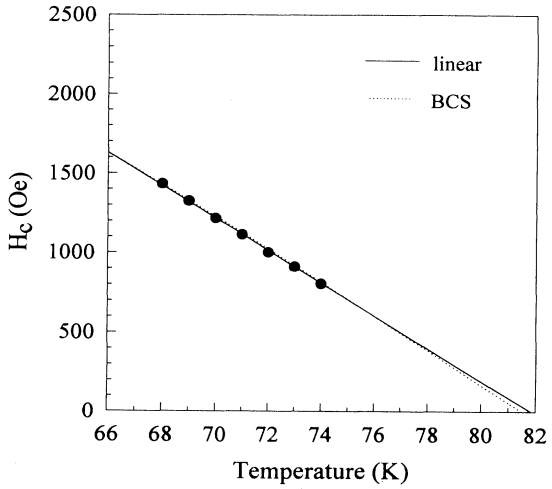

FIG. 5. The temperature dependence of the thermodynamic critical field H_c. BCS temperature dependence of $H_c(T)$ and linear fit are shown. T_c's determined as the x-axis intercepts from both fittings are 81.50 K and 81.85 K.

the onset of fluctuation effects.[6] The abrupt increase of κ near 74 K is thought to be the result of a fluctuation effect.

Another parameter determined from this fitting is the thermodynamic critical field $H_c(T)$, which is shown in Fig. 5. In the limited range from 68 to 74 K, the $H_c(T)$ data are linear in temperature and give $T_c = 81.8$ K and $dH_c/dT = -102.8$ Oe/K. A fit of $H_c(T)$ data to the BCS temperature dependent $H_c(T)$ formula given by Clem,[11] $H_c(T)/H_c(0) = 1.7367[1 - T/T_c][1 - 0.2730(1 - T/T_c) - 0.0949(1 - T/T_c)^2]$, yields $H_c(0) = (0.53 \pm 0.01)\times 10^4$ Oe with $T_c = 81.5$ K. These values are to be compared with the superconducting onset temperature, 81.4 K, measured in low field (5 Oe) M vs T data shown in Fig. 2. Values of the upper critical field derived from $H_{c2} = \kappa\sqrt{2}H_c(T)$ are shown in Fig. 6. From the linear extrapolation of H_{c2}, dH_{c2}/dT and T_c are -1.02 T/K and 81.8 K, respectively. The slope, dH_{c2}/dT, can be also

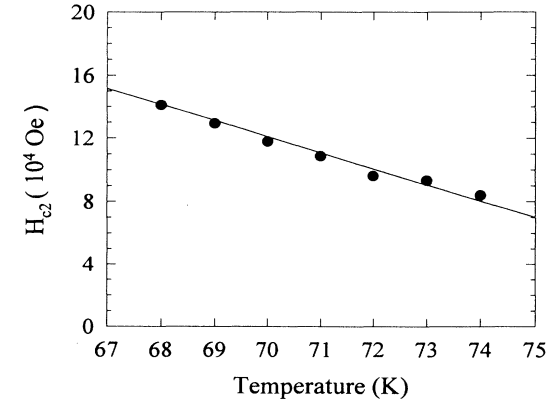

FIG. 6. The temperature dependence of the upper critical field, resulting from the Hao-Clem fitting. The linear slope of H_{c2} below fluctuation region gives $dH_{c2}/dT = -1.02$ T/K.

obtained from the above equation with use of the average κ of 70, which yields $dH_{c2}/dT = -1.018$ T/K near T_c. These values are comparable with each other. Using the approach by Werthamer, Helfand, and Hohenberg (WHH),[12] $H_{c2}(0) \cong -0.7T_c(dH_{c2}/dT)_{T_c}$, which yields $H_{c2}(0) = 58.1$ T. The coherence length ξ can be obtained from the relation $H_{c2}(0) = \phi_0/2\pi\xi^2$ (ϕ_0 is one flux quantum, 2.07×10^{-7} G cm^2) to be 23.8 Å. The penetration depth λ can be derived from the $\kappa = \lambda/\xi$ to be 1666 Å. To see the likely range of λ values it is helpful to use both clean and dirty limit relations. According to the BCS clean limit prediction[13] for $\lambda(T)$, $\lambda(T) = \lambda(0)/\sqrt{2(1-T/T_c)}$ for $T \longrightarrow T_c$, we obtain $\lambda(0) =$ 1879 Å. Meanwhile, in the BCS dirty limit,[13] $\lambda(T) = \lambda(0)/\sqrt{2.7(1-T/T_c)}$ for $T \longrightarrow T_c$, which gives $\lambda(0) =$ 2183 Å. The value of $\lambda(0)$ in the BCS clean limit may be in better agreement with the $\lambda(0)$ value from $\lambda = \kappa\xi$ relation. The lower critical field $H_{c1}(0)$ can be derived from $H_{c1} = (\phi_0/4\pi\lambda^2)(\ln\kappa + 0.5)$ to be 220 Oe.

B. Vortex structure

Because the Hao-Clem model describes the data well, one can derive the values of the vortex core variables that are needed to give the measured magnetization. In the model, the order parameter is written in terms of the

$$f = f_\infty \frac{\rho}{(\rho^2 + \xi_v^2)^{1/2}}, \quad (1)$$

where ρ is the radial distance, f_∞ is the value of f at $\rho = \infty$ and ξ_v governs the rise of f near the core. Once the values of H_c and κ are known, the variational parameters ξ_v and f_∞ can be determined for each value of magnetic field. This order parameter function is independent of the specific vortex structure. Here Hao-Clem introduce the simple vortex structure based on the fact that the triangular array is a close-packed one, in which each vortex is surrounded by a hexagonal array of other vortices. In this structure, the vortex spacing is given[1] as $a = 1.075(\phi_0/H)^{1/2}$. In order to create a Wigner-Seitz-like cell in the vortex structure, the order parameter func-

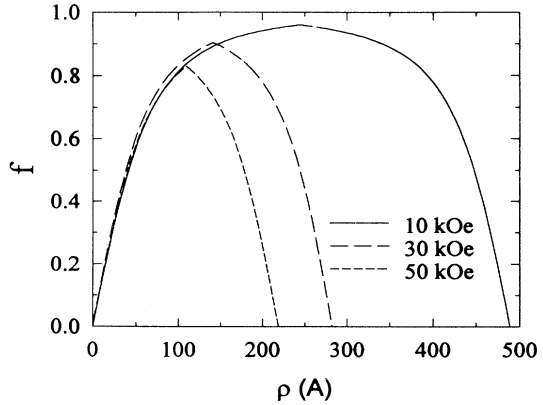

FIG. 7. A simple description for an array of vortices with the order parameter $f(\rho)$ at T = 71 K with the applied fields 1, 3, and 5 T.

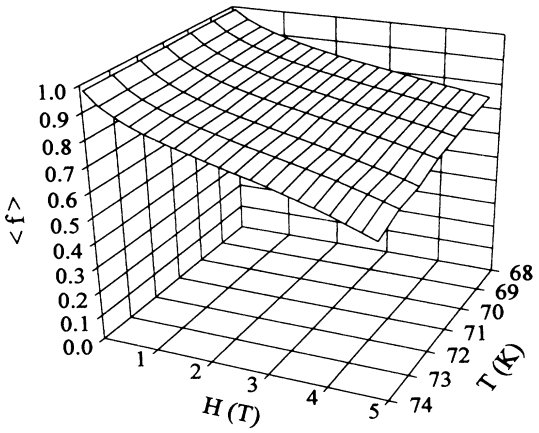

FIG. 8. A plot of the average order parameter $\langle f \rangle$ on the (H, T) plane.

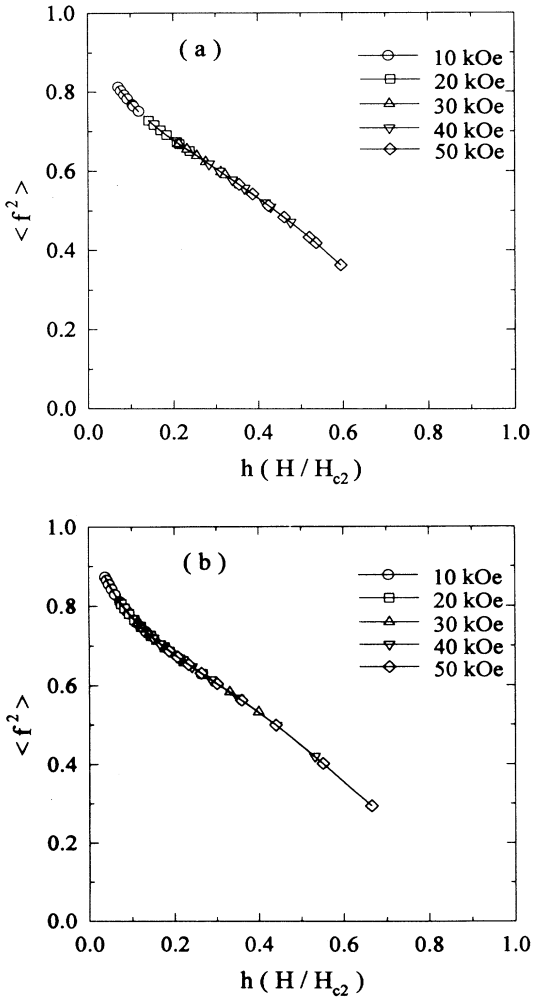

FIG. 9. (a) shows the plot of the Y-124 scaling behavior of $\langle f^2 \rangle$ on a reduced field ($h = H/H_{c2}$) scale. (b) shows the same plot of the Y-123.

tions are cut at the midpoint between vortices, at $a/2$, and symmetrized for the nearest vortex position. Using these values, the order parameter functions derived for an array of vortices at $T = 71$ K with the applied field $H = 1, 3$, and 5 T are shown in Fig. 7. The derivative of the order parameter is discontinuous at the boundary of the Wigner-Seitz-like cell of the vortex. To calculate average values of f and f^2, with the simplification that the unit cell of the vortex array may be approximated by a circular one, we introduce the average order parameter for a single vortex, defined as $\langle f \rangle = (8/a^2) \int_0^{a/2} f(\rho) \rho d\rho$, where a is the vortex spacing. The three-dimensional surface plot of $\langle f \rangle$ on the (H, T) plane is shown in Fig. 8. It shows the supression of the average order parameter by about 58% at 74 K and 5 T.

The density of electrons in the superconducting ground state (n_s) is proportional to $\langle f^2 \rangle$, so we also have evaluated this quantity. Plotting the $\langle f^2 \rangle$ data on a reduced field plot of H/H_{c2} as in Fig. 9, it is clear that the data fall on a universal curve. Here $H_{c2} = \kappa\sqrt{2}H_c(T)$ as derived from fitting the magnetization data. These data are very similar to Y-123 reported previously.[14]

Two conclusions can be drawn from Fig. 9. First, the $\langle f^2 \rangle$ vs H/H_{c2} curves for all temperature and field values fall on a universal curve. Second, this universal curve extrapolates linearly to H/H_{c2} as predicted by Brandt.[10]

C. Fluctuation effect and high field scaling behavior of magnetization

Above 74 K, fluctuation effects become important. A remarkable aspect of the critical fluctuation in high fields is that magnetization is field independent at temperature T^*. Bulaevskii *et al.*[15] and Kogan *et al.*[16] formulated a fluctuation theory in a layered superconductor within a Lowrence-Doniach framework, assuming H is perpendicular to the layers. In Fig. 10, all plots of $4\pi M$ vs T measured at fields between 1 T and 5 T cross at $T^* = 79.2$ K and $4\pi M^* = -0.79$ G. According to a formula, $s = -4\pi k_B T^* / (4\pi M^* \phi_0)$ given by Bulaevskii *et al.*[15] where $4\pi M^*$ is in G and the cgs unit is used, the distance between CuO_2 planes, s, can be estimated to be 8×10^{-7} cm (80 Å). This value of s is larger than one ($\sim$ 10.5 Å) determined by the crystalline structure method. This disagreement may be caused by the application of the two-dimensional (2D) model to a 3D anisotropic superconductor (Y-124). The superconducting volume fraction may be another factor to affect a value of M^* in the above formula. Also the fluctuational diamagnetism above the low-field onset T_c is observed.

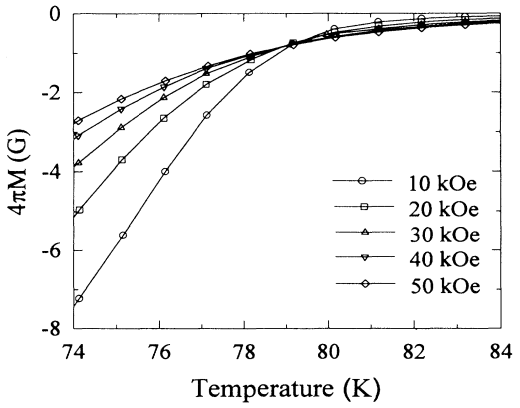

FIG. 10. The temperature dependence of magnetization for c-axis grain-aligned Y-124 with various magnetic fields.

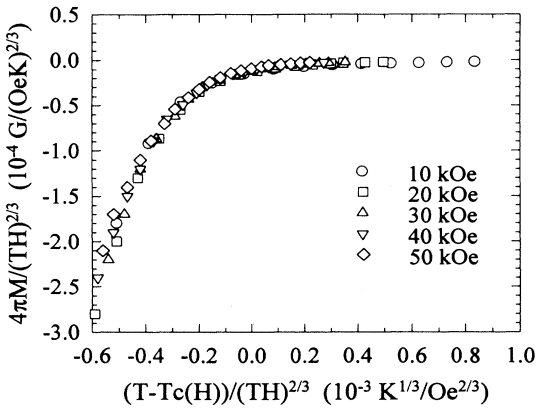

FIG. 11. 3D scaling plot of the magnetization data measured at various magnetic fields.

The temperature and field dependence of magnetization in the transition region in high magnetic fields shows the scaling behavior given by $4\pi M/(TH)^n = F\{A[T - T_c(H)]/(TH)^n\}$, where F is the scaling function, A is a temperature and field independent coefficient, and n is 2/3 for a 3D system and 1/2 for a 2D system. Welp *et al.*[17] showed good 3D scaling behavior for the magnetization, electrical conductivity, Ettinghausen effect, and specific heat of Y-123 single crystals. The 2D scaling behavior was observed by Li *et al.*[18,19] in $Bi_2Sr_2Ca_2Cu_3O_10$ and $Bi_2Sr_2CaCu_2O_8$ single crystals. With two adjustable parameters, T_{c0} and dH_{c2}/dT near T_c, the result of fitting is shown in Fig. 11, where 3D scaling of these magnetization data is displayed. The best fit for 3D behavior yields $T_{c0} \cong 83.0 \pm 0.1$ K and $dH_{c2}/dT \cong -1.9 \pm 0.2$ T/K. Less than a 10% change of dH_{c2}/dT affects a little for the best fit. The 2D scaling behavior of magnetization with any choice of T_{c0} and dH_{c2}/dT shows somewhat poor.

IV. CONCLUSIONS

The reversible magnetization of grain-aligned Y-124 has been studied with the applied fields along the c direction. A successful fitting of the Hao-Clem model to experimental $M(H)$ data gives the results that the GL parameter κ is slightly decreasing up to 72 K, with the value 70 at 71 K, and starts to increase at temperature 73 K. Finally, κ diverges in the vicinity of T_c. The strong fluctuation effects cause this unusual temperature dependence of $\kappa(T)$ near T_c. With the κ value, 70, which

is determined by fitting the data, the derived superconducting parameters are $H_c(0) = 5225$ Oe, $\xi_{ab}(0) = 23.8$ Å, $\lambda_{ab}(0) = 1880$ Å in clean limit, $H_{c1}(0) = 220$ Oe, $H_{c2}(0) = 58$ T, and $dH_{c2}/dT = -1.02$ T/K near T_c.

The spatial average of the order parameter and the square of the order parameter, which uses the Hao-Clem order parameter function, is in good agreement with Brandt's rather well. The plot on $\langle f^2 \rangle$ vs H/H_{c2} shows a universal curve which varies linearly in H/H_{c2} for both Y-123 and Y-124.

The strong fluctuation effects are observed by the crossover of various $4\pi M(T)$ data due to the increasing fluctuational diamagnetism with regard to increasing applied fields. The magnetization data in high fields show good 3D scaling behavior in the variable $[T - T_c(H)]/(TH)^{2/3}$.

ACKNOWLEDGMENTS

The authors are thankful to Z. Hao for useful discussions. Ames Laboratory is operated for the U.S. Department of Energy by Iowa State University under Contract No. W-7405-ENG-82 and supported by the DOE, the Office of Basic Energy Sciences. The work at Northern Illinois University was supported by the NSF through the Science and Technology Center for Superconductivity under Contract No. DMR 91-20000.

* Present address: Samsung Advanced Institute of Technology, Suwon, Korea 440-600.

[1] M. Tinkham, *Introduction to Superconductivity* (McGraw-Hill, New York, 1975).
[2] A. A. Abrikosov, Zh. Eksp. Teor. Fiz. **32**, 1442 (1957) [Sov. Phys. JETP **5**, 1174 (1957)].
[3] U. Welp, W. K. Kwok, G. W. Crabtree, K. G. Vandervoort, and J. Z. Liu, Phys. Rev. Lett. **62**, 1908 (1989).
[4] Z. Hao, J. R. Clem, M. W. McElfresh, L. Civale, A. P. Malozemoff, and F. Holtzberg, Phys. Rev. B **43**, 2844 (1991).
[5] Z. Hao and J. R. Clem, Phys. Rev. Lett. **67**, 2371 (1991).
[6] J. Gohng and D. K. Finnemore, Phys. Rev. B **46**, 398 (1992).
[7] D. E. Morris, N. G. Asmar, J. H. Nickel, R. L. Sid, and J. Y. T. Wei, Physica C **159**, 287 (1989).
[8] W. C. Lee and D. M. Ginsberg, Phys. Rev. B **45**, 7402 (1992).
[9] G. Triscone, A. F. Khoder, C. Opagiste, J.-Y. Genoud, T. Graf, E. Janod, T. Tsukamoto, M. Couach, A. Junod, and J. Muller, Physica C **224**, 263 (1994).
[10] E. H. Brandt, Phys. Status Solidi B **51**, 345 (1972).
[11] J. R. Clem, Ann. Phys. (N.Y.) **40**, 268 (1966).
[12] N. R. Werthamer, E. Helfand, and P. C. Hohenberg, Phys. Rev. **147**, 295 (1966).
[13] A. A. Abrikosov, L. P. Gor'kov, and I. Y. Dzyaloshinskii, *Quantum Field Theoretical Methods in Statistical Physics*, (Pergamon, Oxford, 1965).
[14] Junho Gohng, Ph.D. dissertation, Iowa State University, 1992.
[15] N. L. Bulaevskii, M. Ledvij, and V. G. Kogan, Phys. Rev. Lett. **68**, 3773 (1992).
[16] V. G. Kogan, M. Ledvij, A. Yu. Simonov, J. H. Cho, and D. C. Johnston, Phys. Rev. Lett. **70**, 1870 (1993).
[17] U. Welp, S. Fleshler, W. K. Kwok, R. A. Klemm, V. M. Vinokur, J. Downey, B. Veal, and G. W. Crabtree, Phys. Rev. Lett. **67**, 3180 (1991).
[18] Q. Li, M. Suenaga, T. Hikata, and K. Sato, Phys. Rev. B **46**, 5857 (1992).
[19] Q. Li, K. Shibutani, M. Suenaga, I. Shigaki, and R. Ogawa, Phys. Rev. B **48**, 9877 (1993).